Materials Science & Engineering A 626 (2015) 369–374

Contents lists available at ScienceDirect

Materials Science & Engineering A

journal homepage: www.elsevier.com/locate/msea

β Zr–Nb–Ti–Mo–Sn alloys with low Young's modulus and low magnetic susceptibility optimized via a cluster-plus-glue-atom model

Chang Pang [a], Qing Wang [a,*], Ruiqian Zhang [b], Qun Li [a], Xun Dai [b], Chuang Dong [a], Peter K. Liaw [c]

[a] Key Laboratory of Materials Modification by Laser, Ion and Electron Beams (Ministry of Education), School of Materials Science and Engineering, Dalian University of Technology, Dalian 116024, China
[b] Science and Technology on Reactor Fuel and Materials Laboratory, Nuclear Power Institute of China, Chengdu 610041, China
[c] Department of Materials Science and Engineering, The University of Tennessee, Knoxville, TN 37996, USA

ARTICLE INFO

Article history:
Received 26 November 2014
Received in revised form
19 December 2014
Accepted 23 December 2014
Available online 31 December 2014

Keywords:
Zr–Ti–Mo–Sn–Nb alloys
Alloy design
Phase transformations
Mechanical properties
Magnetic properties

ABSTRACT

The multi-element Zr-based bio-alloys are optimized for reaching lower Young's modulus and magnetic susceptibility by introducing the cluster-plus-glue-atom model to realize the composition design. A general cluster formulas of $[(Mo,Sn)–(Zr,Ti)_{14}]Nb_x$ ($x=1, 3$) was obtained from the model and alloy rods with a diameter of 3 mm were prepared by copper-mold suction-casting processing. The β structural stabilities of the designed alloys were studied by the valence electron concentration (*VEC*). Among the β-Zr alloys, the $[(Mo_{0.5}Sn_{0.5})–Zr_{14}]Nb_1$ ($Zr_{87.5}Nb_{6.25}Mo_{3.13}Sn_{3.13}$ at%) and $[(Mo_{0.5}Sn_{0.5})–(Zr_{13}Ti)]Nb_1$ ($Zr_{81.25}Nb_{6.25}Ti_{6.25}Mo_{3.13}Sn_{3.13}$ at%) alloys, corresponding to the lower β stability limit, display lower Young's moduli (77–79 GPa), lowest magnetic susceptibilities (2.12×10^{-6}–2.13×10^{-6} $cm^3\ g^{-1}$), as well as higher Vickers hardness (288–311 HV).

1. Introduction

The Zr–Nb alloys have lower magnetic susceptibilities (χ_g) than other biomaterials, such as in Co–Cr–Mo and Ti–Al–V systems, which make them suitable as implant materials that allow magnetic resonance imaging diagnostic in surgery [1–6]. Multiple phases, such as α′, β, and ω, often co-existed in the Zr–Nb alloys, where the body-centered cubic structure (BCC) β phase plays a dominant role with increasing the Nb content [7–11]. Especially, the β phase is responsible for the desired low Young's modulus (E) and other properties, while its magnetic susceptibility is relatively high [11–13]. So multi-element alloying could solve this issue and reach an optimum balance between low E and low χ_g through controlling the β stabilities properly. Considering the complexity induced by the multi-element alloying, effective alloy design methods are generally required to reach the optimized alloying effects [14–16].

In the present work, a cluster-plus-glue-atom model is introduced to design β Zr–Nb–Ti–Mo–Sn alloys with low Young's modulus and low magnetic susceptibility, which was applied into the composition optimization of low-E multi-element β-Ti alloys [17]. This cluster-plus-glue-atom model was proposed on the basis of chemical short-range order between solute atoms and solvent atoms [17,18], and could dissociate an alloy structure into two parts, the cluster part and the glue atom part. Since in the BCC structure the interactions between the solute and solvent atoms exert impacts up to the second-nearest neighbor shells around the solute atoms [19–23], the cluster part can be expressed with a CN14 (CN: coordination number) rhombi-dodecahedral cluster, as shown in Fig. 1, consisting of eight solvent atoms of the first-nearest neighbor shell and six solvent atoms of the second-nearest neighbor shell. Such clusters are generally formed in the solute elements with large negative enthalpies of mixing ΔH with the base element, while the glue atoms situate at the interstitial sites between clusters to serve the linkage, exhibiting weakly negative or positive ΔH values with the base element. Thus, the BCC structure is described with a simple universal cluster formula of $[(\text{center atom})–(\text{shell atom})_{14}](\text{glue atom})_x$, x being the integer number of glue atoms matching one cluster. A series of β-Ti bio-alloys have been developed in light of this model [17,24], and the general cluster formula, $[(Mo,Sn)–(Ti,Zr)_{14}]Nb_1$, can lead to both lower BCC stability limit and lower E simultaneously. Note that all the cluster formulas in the paper are expressed with atomic fraction. In analogy to this trend, the same universal cluster formula $[(Mo,Sn)–(Zr,Ti)_{14}]Nb_x$ is determined in the Zr-based systems in light of ΔH between solute atoms with the base Zr

* Corresponding author. Tel.: +86 411 84708615; fax: +86 411 84708389.
E-mail address: wangq@dlut.edu.cn (Q. Wang).

http://dx.doi.org/10.1016/j.msea.2014.12.082
0921-5093/

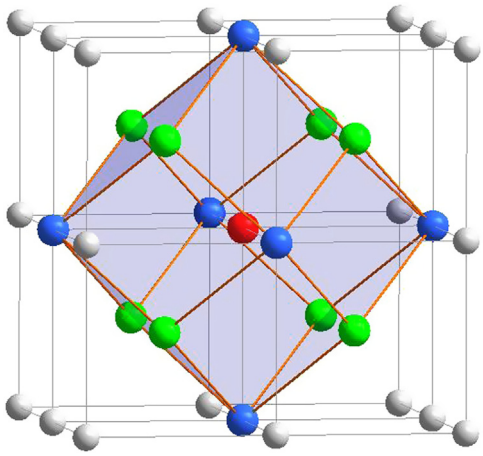

Fig. 1. The CN14 rhombi-dodecahedral cluster, which consists of eight solvent atoms of the first-nearest neighbor shell (green balls) and six solvent atoms of the second-nearest neighbor shell (blue balls). The red ball represents the cluster center atom. (For interpretation of the references to color in this figure legend, the reader is referred to the web version of this article.)

Table 1
Basic parameters of alloying elements, including the crystal structure, number of valence electrons, N, enthalpy of mixing, ΔH_{Zr-M}, between the solutes, M, and solvent, Zr, Young's modulus, E, and magnetic susceptibility, χ_g [26].

Element	Crystal structure	N	ΔH_{Zr-M} (kJ mol^{-1})	E (GPa)	χ_g (10^{-6} cm^3 g^{-1})
Zr	HCP&BCC	4	–	68	1.32
Nb	BCC	5	4	105	2.24
Mo	BCC	6	−6	329	0.75
Ti	HCP&BCC	4	0	116	3.15
Sn	Tetragonal	4	−43	50	0.03

HCP represent hexagonal close-packed structure in the table.

[25], i.e., Mo and Sn taken as the cluster center atoms due to the negative ΔH_{Zr-Mo} (−6 kJ mol^{-1}) and ΔH_{Zr-Sn} (−43 kJ mol^{-1}) (seen in Table 1), Ti replacing the base Zr on the cluster shell due to the zero ΔH_{Zr-Ti}, and Nb as the glue atom due to the positive ΔH_{Zr-Nb} (4 kJ mol^{-1}). Therefore, the present paper will investigate the structural stability, mechanical properties, and magnetic susceptibilities of the Zr–Ti–Mo–Sn–Nb alloys developed on the basis of the cluster formula [(Mo,Sn)–(Zr,Ti)$_{14}$]Nb$_x$.

2. Composition design

Table 1 lists the basic parameters of the alloy elements involved. Among them, the values of Young's modulus (E) and magnetic susceptibility (χ_g) are opposite for BCC β-stabilized elements Nb, Mo, and Ti. Sn has both a low E and a low χ_g, but is a weak β stabilizer. To reach a desired combination of properties, i.e., the sufficient BCC stability (to guarantee a single β phase), low E and low χ_g simultaneously, these elements should be optimized, and the suggested cluster formula will serve the basis of the alloy design.

In the basic binary Zr–Nb system, the cluster formula for stable solid solutions should be formulated as [Zr–Zr$_{14}$]Nb$_x$ to constitute the basic formula for further alloying, where Zr atoms form the cluster by themselves due to the positive ΔH_{Zr-Nb}=4 kJ mol^{-1} [25]. The number of glue atoms Nb could be readily obtained by fitting the known Zr–Nb alloys with the formulas. Some typical binary Zr–Nb alloys as listed in Table 2 can well be explained with the [Zr–Zr$_{14}$] plus one, three, and four Nb atoms. For instance, the formula [Zr–Zr$_{14}$]Nb$_1$ with Zr–6.4Nb (weight percent, wt%) can explain the composition of Zr–6Nb alloy that is known for a very low χ_g and a relatively low E [11]. The [Zr–Zr$_{14}$]Nb$_3$ with Zr–16.9Nb (wt%) could explain the Zr–16Nb alloy, which shows the moderate tensile strength and elongation [11]. In addition, the cluster formula [Zr–Zr$_{14}$]Nb$_4$ (Zr–21.4Nb wt%) falls close to the Zr–22Nb alloy with the best electrochemical performance and good biocompatibility [12].

Thus, on the basis of the binary cluster formulas of [Zr–Zr$_{14}$]Nb$_x$ (x=1, 3), multi-alloying with Mo, Ti and Sn can be achieved by substitutions, leading to [(Mo,Sn)–(Zr,Ti)$_{14}$]Nb$_x$ (x=1, 3). The so-designed alloys are expected to show low Young's moduli, sufficient β structural stabilities, and low magnetic susceptibilities simultaneously because the atoms are all properly configured within the framework of the cluster formula. Table 3 lists all the designed cluster formulas, including their atomic percent (at%) and weight percent (wt%).

3. Experimental procedure

The alloy ingots of designed [(Mo,Sn)–(Zr,Ti)$_{14}$]Nb$_x$ (x=1, 3) were prepared by arc-melting the mixtures of Zr, Ti, and Mo with a purity of 99.99%, as well as Nb and Sn with 99.95% in the Ti-gettered high-purity argon atmosphere. The ingots were flipped and remelted at least three times to ensure the chemical homogeneity. The furnace was evacuated to less than 8×10^{-3} Pa and was then filled with the pure argon. Cylindrical rods with 3 mm in diameter were prepared by copper-mold suction-casting. The mass loss was controlled below 0.1% in the whole process. Structural identification was performed by the Bruker X-ray diffraction (XRD) using the Cu K_α radiation (λ=0.15406 nm). The morphology and phase verification were further observed using the Philips Tecnai G^2 transmission electron microscopy (TEM) with the selected-area electron-diffraction (SAED) analysis. The TEM samples were prepared by twin-jet electro-polishing in a solution containing 60% CH_3OH+34% $CH_3(CH_2)_3OH$+6% $HClO_4$ (volume fraction) at −30 °C. The Young's modulus, E, and nanoindentation hardness, H_{IT}, of the alloys were measured by a MTS nanoindenter XP system at room temperature. The maximum indentation depth was controlled at 2 μm. The Vickers hardness, HV, was carried out using HVS-1000 Vickers indenter under a load of 200 g with 15 s. Each sample was measured at least 8 times and the averaged value is taken. Magnetic susceptibility, χ_g, was measured at 300 K, using the Magnetic Property Measurement System (MPMS) XL-7 by the Quantum Design Company, where the magnetic field strength was controlled at 1000 Oe.

4. Results and discussions

Fig. 2 shows the XRD patterns of [(Mo,Sn)–(Zr,Ti)$_{14}$]Nb$_x$ (x=1, 3) alloy series. In the alloy series with x=1 [Fig. 2(a)], besides β, the peaks originated from the α and ω phases, were detected in the alloys [Zr–Zr$_{14}$]Nb$_1$, [Ti–Zr$_{14}$]Nb$_1$ and [Sn–Zr$_{14}$]Nb$_1$, showing the instabilities of a β structure caused by the absence of Mo and by insufficient Nb. The other three alloys with Mo, [Mo–Zr$_{14}$]Nb$_1$, [(Mo$_{0.5}$Sn$_{0.5}$)–Zr$_{14}$]Nb$_1$, and [(Mo$_{0.5}$Sn$_{0.5}$)–(Zr$_{13}$Ti)]Nb$_1$, exhibit a single BCC-β phase. While all the alloys with x=3 appear to be a single BCC structure [Fig. 2(b)]. Since the binary [Zr–Zr$_{14}$]Nb$_3$ is already a pure BCC alloy, the multi-component alloys with three Nb atoms should possess a quite stable BCC structure.

Although some alloys possess a single BCC structure from the XRD diffraction peaks, a minor amount of second precipitations could be unveiled in some Sn-added β-Zr alloys with TEM. Fig. 3 shows the TEM observations of the β-Zr alloys of [(Mo$_{0.5}$Sn$_{0.5}$)–Zr$_{14}$]Nb$_1$ and [(Mo$_{0.5}$Sn$_{0.5}$)–(Zr$_{13}$Ti)]Nb$_1$. The SAED analysis shows that weak diffraction spots of α″ and ω phases are detected besides